International Journal of Electrical and Computer Engineering (IJECE)
Vol. 15, No. 2, April 2025, pp. 1487~1498
ISSN: 2088-8708, DOI: 10.11591/ijece.v15i2.pp1487-1498

Vehicle side control of a wireless power transfer charger using optimized artificial neural network

Marouane El Ancary, Abdellah Lassioui, Hassan El Fadil, Anwar Hasni, Yassine El Asri, Zakariae El Idrissi
Ingénerie des Systèmes Avancés (ISA) Laboratory, National School of Applied Sciences (ENSA), Ibn Tofail University, Kenitra, Morocco

Article Info

Article history:

Received Jul 26, 2024
Revised Oct 25, 2024
Accepted Nov 20, 2024

Keywords:

Artificial intelligence
Artificial neural network
Electric vehicles
Vehicle side control
Wireless power transfer

ABSTRACT

This paper investigates a new approach to control a wireless power transfer (WPT) charger for electric vehicles (EVs) employing an optimized artificial neural network (ANN). Enhancing the efficiency and robustness of such systems is crucial, and integrating artificial intelligence (AI)-based solutions has introduced innovative approaches in this field. The proposed method enables precise regulation of battery charging voltage even under challenging conditions, such as coil misalignment or shared grounding assemblies for multiple EVs. To assess the stability and robustness of the proposed controller, its performance was evaluated under scenarios of coil misalignment and shared grounding assemblies for EVs with varying battery voltages. The controller effectively eliminated overshoot and significantly reduced residual output voltage ripple by 4.33% compared to a conventional proportional-integral (PI) controller, demonstrating the superior performance and reliability of the ANN-based control approach.

Corresponding Author:

Marouane El Ancary
Ingénerie des Systèmes Avancés (ISA) Laboratory, National School of Applied Sciences (ENSA), Ibn Tofail University
Campus Universitaire, B.P 241, Kenitra 14000, Morocco
Email: marouane.elancary@gmail.com

1. INTRODUCTION

The transportation sector is a primary contributor to climate change, with the combustion of fossil fuels in vehicles releasing substantial quantities of carbon dioxide. This greenhouse gas exacerbates global warming, leading to increasingly frequent and severe weather events [1]. Road transportation, particularly passenger vehicles, is a dominant source of these emissions, though aviation and maritime transport also contribute significantly. Transitioning to sustainable modes of transportation, such as public transit, cycling, and walking, coupled with the development of cleaner vehicle technologies, is essential for mitigating climate change impacts [2], [3]. Electric vehicles (EVs) offer a promising solution to decarbonize the transportation sector. EVs drastically reduce greenhouse gas emissions by replacing fossil fuels with electricity, often generated from renewable sources. The absence of tailpipe emissions improves air quality and mitigates climate change effects. Furthermore, battery technology advancements have enhanced EVs' economic viability, accelerating their adoption as a sustainable transportation alternative [4]. However, to maximize the benefits of EVs, it is essential to develop appropriate recharging infrastructures and solve the problems of autonomy and battery longevity. Among recent innovative approaches, wireless charging systems seem particularly promising for their ability to make recharging more convenient and accessible [5].

Wireless power transfer (WPT) technology offers a convenient and efficient method for charging EVs without the need for physical connections [6]. This technology, based on magnetic induction, enhances safety by eliminating the risks associated with traditional charging methods, such as electric shocks and fires caused by exposed cords [7]. Furthermore, WPT facilitates automated charging, improving user convenience. Due to their reliability, durability, and resistance to adverse weather conditions, wireless EV chargers are particularly suitable for locations with restricted access [8], [9]. Figure 1 shows a simplified WPT system comprises two different main parts: the vehicle-side part and the ground-side part [10]. Energy transfer occurs wirelessly through a magnetic field generated by an underground transmitting coil and received by a coil positioned beneath the vehicle [11], [12]. To ensure efficient energy transfer to the electric vehicle battery, a control system is necessary to regulate the energy flow.

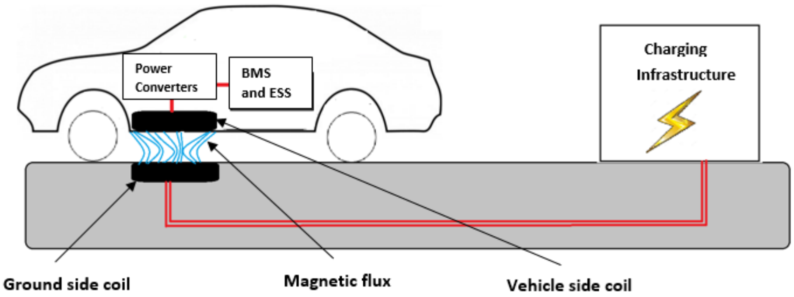

Figure 1. Simplified configuration of a WPT charging system

There are three methods to control WPT chargers: primary-side, secondary-side, and dual-side control [13]. Each approach regulates voltage and current, either on the ground side, the vehicle side, or a combination of both. For vehicle-side control, [14] presents a closed-loop strategy utilizing bidirectional switches modulated by a proportional-integral (PI) controller. This method regulates output current and voltage during battery charging, enabling both constant current (CC) and constant voltage (CV) phases. Also, a comparative study of two secondary-side control techniques, PI and one-cycle control (OCC), is presented for WPT chargers [15]. The effectiveness of these methods in maintaining power regulation is assessed under varying mutual inductance conditions. Bhavsingh *et al.* [16] propose a WPT charger to maximize power transmission. Their approach involves using duty cycle control based on the fundamental harmonic approximation method. To achieve this, they incorporate two bidirectional switches before the rectifier on the vehicle side of the system. The proposed control strategy in [17] employs a boost converter on the vehicle side with duty cycle modulation to achieve CC and CV charging phases. In [18], a semi-bridgeless active rectifier controlled by a PI regulator is employed on the secondary-side to regulate the output voltage. Pulse density modulation is implemented for the active rectifier switches to enhance converter efficiency. In [19], a nonlinear H-infinity controller is employed for the secondary-side DC-DC converter. To optimize controller parameters during variable voltage intermittent charging, a multi-objective, multi-constraint algorithm is utilized. All previous studies have employed secondary-side control based on either PI or non-linear controllers.

While PI controllers are simple to implement, they are ill-suited for highly nonlinear systems such as power converters in WPT chargers. Nonlinear controllers, on the other hand, offer superior performance for such systems but often require additional sensors, increasing both cost and complexity. Most existing research focuses on voltage and current regulation due to misalignment issues in WPT systems. Moreover, there is a notable gap in the literature regarding shared ground assemblies for charging multiple electric vehicle batteries. Additionally, the potential of artificial intelligence in controlling these complex systems remains largely unexplored, highlighting a need for further investigation in this area.

This paper introduces a novel vehicle-side control technique for WPT chargers designed for EVs. This technique leverages an optimized artificial neural network to achieve two primary objectives. First, it enables the charging of two distinct battery types with different voltages using a single charging station or ground-side assembly. Second, it maintains a constant battery charge, even in the presence of voltage fluctuations caused by coil misalignment or grid instability on the primary side of the WPT charger.

The remaining sections of this document are organized as follows: section 2 introduces the WPT charger, its modeling, and the equivalent circuit representation. Section 3 illustrates the proposed control strategy. Section 4 presents the results and discussion of the control technique and its performance based on simulation results. Finally, section 5 presents conclusions and future research directions.

2. WIRELESS POWER TRANSFER CHARGER

2.1. Principle of operation of the WPT

This section is devoted to the description of the WPT charger. The cable-free charging process is schematically summarized in the SAE J2954 standard and may be divided into two subsystems, as Figure 2 illustrates: the primary side, also known as the ground assembly (GA), and the secondary side, also known as the vehicle assembly (VA) [20]. A high-frequency DC/AC converter, operating at 85 kHz as recommended in SAE J2954 standard, generates a time-varying voltage. The transmitting coil, energized by the inverter, generates a time-varying magnetic field (MF). This MF is transmitted wirelessly and carried to the receiving coil [21], [22]. The normalized voltages and currents required by the battery are obtained by rectifying the voltage from the secondary coil [23].

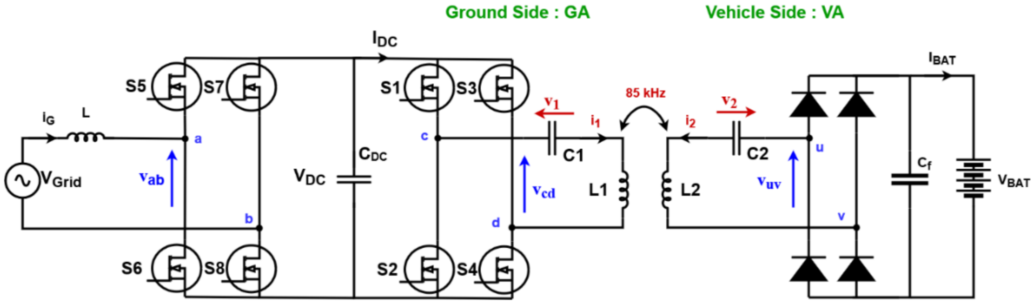

Figure 2. Wireless power transfer charger circuit

2.2. Modeling of the WPT

This section focuses on developing a precise analytical model for the wireless charger, excluding the AC/DC power factor correction (PFC) converter stage. The analysis is confined to the system components between the DC bus and the vehicle battery. Furthermore, the battery is modelled by a resistor r_b in series with an open circuit voltage v_{OC}. Once Kirchhoff's rules are applied to the circuit in Figure 2, the results are shown in (1) – (5):

$$v_{CD} = v_1 + L_1 \frac{di_1}{dt} - M\frac{di_2}{dt} \quad (1)$$

$$M\frac{di_1}{dt} = v_{uv} + v_2 + L_2\frac{di_2}{dt} \quad (2)$$

$$i_1 = C_1\frac{dv_1}{dt} \quad (3)$$

$$i_2 = C_2\frac{dv_2}{dt} \quad (4)$$

$$i_{BAT} = |i_2| = \frac{v_0 - v_{OC}}{r_b} + C_f\frac{dv_0}{dt} \quad (5)$$

Where, i_1 and i_2 are the currents in the primary side and secondary side coils, L_2 and L_2 are the inductances of the primary and secondary side coils, M is the mutual inductance between the coils, v_{cd} is the inverter output voltage, v_1 and v_2, are, respectively, the voltage across the primary and secondary side compensation capacitors, v_{uv} and v_0 are, respectively, the voltage at the input and output of the secondary side rectifier, and C_f is the filtering capacitor of the secondary side [24].

From (1) to (5), the following state space model is obtained:

$$x = [v_1, v_2, i_1, i_2, v_0]^T = [x_1, x_2, x_3, x_4, x_5]^T \quad (6)$$

$$\dot{x}_1 = \frac{1}{C_1}x_3 \quad (7)$$

$$\dot{x}_2 = \frac{1}{C_2}x_4 \quad (8)$$

$$\dot{x}_3 = \frac{1}{K_1}(v_{cd} - x_1) - \frac{1}{K_2}(x_2 - sgn(x_4)x_5) \quad (9)$$

$$\dot{x}_4 = \frac{1}{K_2}(v_{cd} - x_1) - \frac{1}{K_3}(x_2 - sgn(x_4)x_5) \quad (10)$$

$$\dot{x}_5 = \frac{1}{C_f} sgn(x_4)x_4 - \frac{x_5 - v_{OC}}{C_f r_b} \quad (11)$$

Where $K_1 = \frac{L_1L_2 - M^2}{L_2}$, $K_2 = \frac{L_1L_2 - M^2}{M^2}$, $K_3 = \frac{L_1L_2 - M^2}{L_1}$ and $sgn(x) = 1$ when $x > 0$, $sgn(x) = -1$ when $x < 0$ and $sgn(x) = 0$ when $x = 0$.

3. CONTROLLER DESIGN

The purpose of this section is to design a controller for the WPT system. A buck-boost DC-DC converter will enable the battery voltage to be controlled only in constant voltage (CV) mode. The use of the artificial neural network in this control technique will make it possible to achieve the objectives of regulation in the presence of fluctuation of the vehicle side input voltage due to misalignment between the coils and also to enable two batteries of two different voltages to be charged with the same ground side assembly. Figure 3 shows the fundamental principle of the proposed control method. To evaluate the controller's robustness under various operating conditions, the battery is replaced with a variable load resistor.

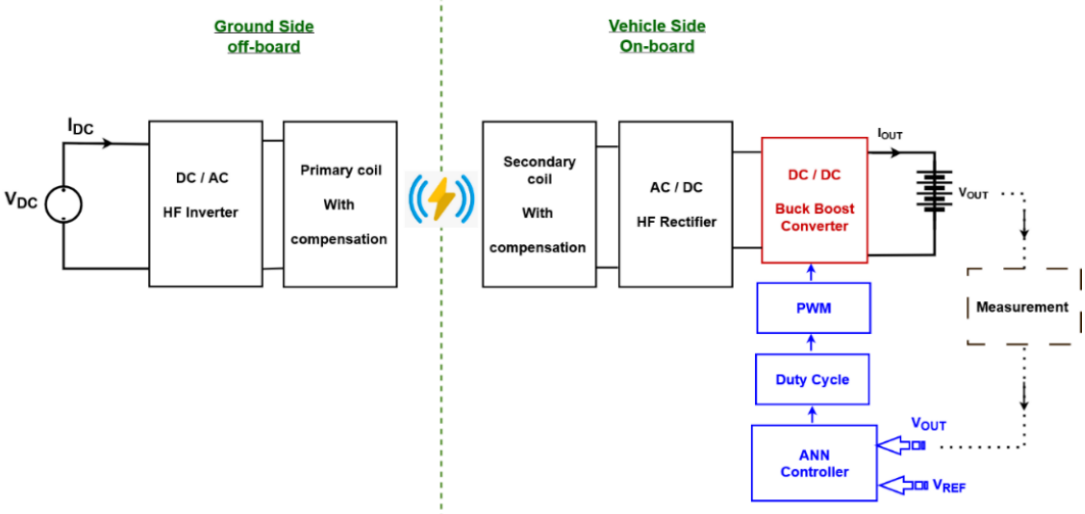

Figure 3. Fundamental principle of the proposed control approach

3.1. Buck-Boost DC-DC converter

The buck-boost converter aims to precisely regulate output voltage by tracking a reference value. This is achieved by modulating the converter's duty cycle [25]. The buck-boost converter topology is depicted in Figure 4. Kirchhoff's rules can be applied to the circuit analysis in order to obtain the (12) and (13), assuming initially that S = 1. Where r_L and r_S represent, respectively, the inductor's equivalent series resistance and the power switch's resistance.

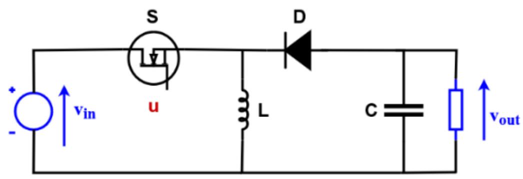

Figure 4. Buck Boost DC-DC converter circuit

$$\frac{di_L}{dt} = -\frac{r_L + r_S}{L} i_L + \frac{V_{in}}{L} \tag{12}$$

$$\frac{dV_{out}}{dt} = -\frac{V_{out}}{RC} \tag{13}$$

The switch is OFF (S = 0) while the diode is conducting, producing the following result (14) and (15).

$$\frac{di_L}{dt} = -\frac{r_L}{L} i_L - \frac{V_{out}}{L} \tag{14}$$

$$\frac{dV_{out}}{dt} = -\frac{i_L}{C} - \frac{V_{out}}{RC} \tag{15}$$

The variable x, which comprises the inductor current and the output voltage, is included in the state vector of the circuit, as depicted in (16).

$$\begin{pmatrix} \frac{di_L}{dt} \\ \frac{dv_{out}}{dt} \end{pmatrix} = \begin{pmatrix} \dot{x}_1 \\ \dot{x}_2 \end{pmatrix} = \begin{pmatrix} -\frac{r_L + r_S}{L} d - -\frac{r_L}{L}(1-d) & -\frac{1}{L}(1-d) \\ \frac{-1}{C}(1-d) & -\frac{1}{RC} \end{pmatrix} \begin{pmatrix} x_1 \\ x_2 \end{pmatrix} + \begin{pmatrix} \frac{d}{L} \\ 0 \end{pmatrix} V_{in} \tag{16}$$

Finally, the relationship between V_{in} and V_{out} is given in (17).

$$\frac{V_{out}}{V_{in}} = \frac{d}{1-d} \tag{17}$$

3.2. Artificial neural network model

The artificial neural network (ANN) model is inspired by the functioning of biological neurons. In contrast to traditional algorithms, ANNs learn from input data and transform it into knowledge in a manner like to that of the human brain. ANNs are architecturally formed by interconnected elementary units named neurons. The structure of neural networks commonly follows a layered structure. The network architecture is defined by the number of layers and the number of neurons within each layer [26].

The controller model used in this paper is founded on a feedforward ANN as illustrated in Figure 5, feedforward ANNs are renowned for their simplicity, efficiency, and ease of training, making them well-suited for various tasks, including control systems. The buck-boost DC-DC converter's input voltage and the simulated battery reference voltage, represented by the load resistance, serve as inputs to the neural network. The model's output, the duty cycle “d”, directly controls the output voltage. The ANN model dynamically adjusts the duty cycle based on input conditions to accurately track the desired reference, thereby controlling the converter's operation in either boost or buck mode. The architecture of the ANN is shown in Figure 5(a) consists of three separate layers: the input layer, the hidden layer which contains 25 neurons, and the output layer. It has two inputs and one output. Figure 5(b) shows the layers of the neural network. Weights and biases are the parameters an ANN learns during training to minimize errors between the network's output and the desired output.

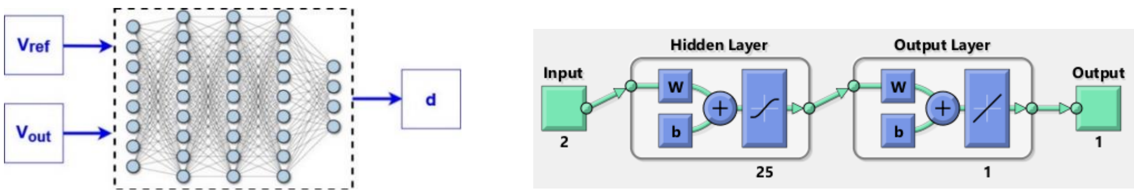

(a) (b)

Figure 5. Feedforward ANN: (a) architecture and (b) layers of the ANN

Mean squared error (MSE) is a widely used metric to evaluate the performance of machine learning models, including ANNs. A lower MSE generally indicates a better-performing model because it can minimize prediction errors, prevent overfitting, and generalize well to new data. By optimizing the training process to minimize MSE, ANN models can achieve higher accuracy and reliability. In this context, a comparative analysis was conducted using three training algorithms: Levenberg-Marquardt, Bayesian Regularization, and scaled conjugate gradient to select the optimal ANN model. The results of this evaluation are summarized in Tables 1, 2, and, 3. The Levenberg-Marquardt algorithm yielded the lowest error and the highest regression coefficient, demonstrating superior performance in training the ANN model compared to the other considered algorithms.

Table 1. Learning results using the Levenberg-Marquardt algorithm

Phase	Samples	MSE	Regression (R)
Training	10501	1.10102×10^{-9}	9.99999×10^{-1}
Validation	2250	5.62882×10^{-1}	9.99999×10^{-1}
Testing	2250	9.71649×10^{-1}	9.99999×10^{-1}

Table 2. Learning results using the Bayesian Regularization algorithm

Phase	Samples	MSE	Regression (R)
Training	10501	2.09661×10^{-8}	9.99996×10^{-1}
Validation	2250	0.00000×10^{-0}	0.00000×10^{-0}
Testing	2250	3.23009×10^{-9}	9.99999×10^{-1}

Table 3. Learning results using the scaled conjugate gradient algorithm

Phase	Samples	MSE	Regression (R)
Training	10501	7.15706×10^{-7}	9.99865×10^{-1}
Validation	2250	8.19750×10^{-7}	9.99864×10^{-1}
Testing	2250	8.18438×10^{-7}	9.99844×10^{-1}

The ANN model was evaluated using the Levenberg-Marquardt algorithm. Figure 6 illustrates the learning performance of the optimized ANN-based controller. The mean squared error (MSE) reached a minimum value of 1.4485×10^{-9} at epoch 41, indicating successful convergence. The close alignment of the learning, testing, and validation curves suggests that the ANN model exhibits strong generalization capabilities. The effectiveness of the control approach has been evaluated. The simulation parameters are detailed in Table 4.

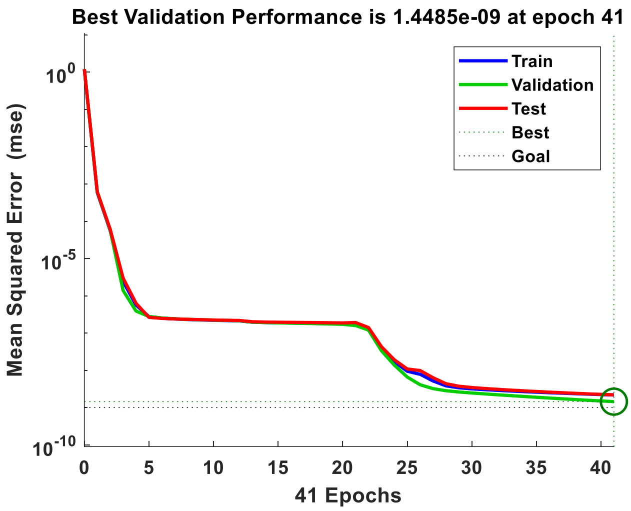

Figure 6. Learning performance of the optimized ANN-based controller

Table 4. Parameters used during the simulation

Parameter	Value
DC bus voltage for primary side VDC	200 V
Self-inductance of the ground side coil L1	416 µH
Self-inductance of the vehicle side coil L2	116 µH
Mutual inductance M	20 µH
Primary side compensation capacitor C1	8.5 nF
Secondary side compensation capacitor C2	30 nF
Resonance frequency f	85 kHz
Inductor of the DC-DC converter L	500 µH
Capacitor of the DC-DC converter C	1 mF
Input voltage of the DC-DC converter	60 V
Switching frequency	10 KHz

4. RESULTS AND DISCUSSION

This section presents a comparative analysis of the tracking performance of the ANN-based control technique and a traditional PI controller. To evaluate the stability and robustness of the new approach, various scenarios were considered. The first scenario involved charging two vehicles with different battery voltages using a common ground assembly to assess the method's versatility. The second scenario focused on maintaining a constant output voltage under input voltage fluctuations on the vehicle side, simulating potential misalignment or grid instability issues.

4.1. Tracking test of the control technique

To evaluate the ANN controller's performance, a tracking test was conducted. Initially, a 60 V reference voltage is applied, simulating the load's voltage demand. After two seconds, this reference is increased to 80 V. Figure 7 presents a comparative analysis of the proposed controller's and the conventional PI controller's performance. Both controllers successfully track and stabilize at the desired setpoint. The PI controller exhibited significant overshoot, reaching 111 V for a 60 V reference (an 85% overshoot), and sustained a 5.66% residual ripple as shown in Figure 7(a), such oscillations compromise the battery charging system's constant voltage operation and can introduce system instabilities. In contrast, the ANN-optimized controller exhibits no overshoot at any output voltage level, as evidenced in Figure 7(b). The absence of overshoot is a critical advantage of the ANN controller, particularly for electric vehicle battery charging where battery health is paramount. Additionally, the ANN controller effectively diminishes residual ripple to approximately 1.33% of the final output value.

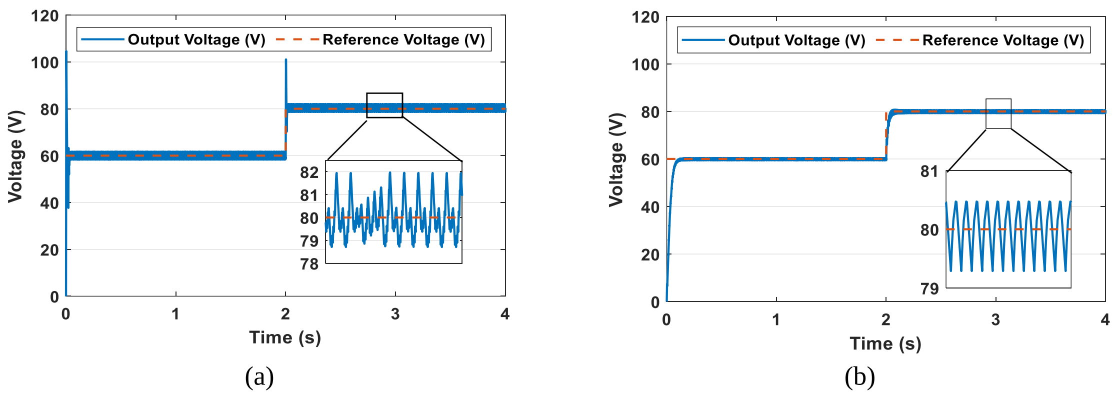

Figure 7. Reference voltage and output voltage using: (a) PI controller and (b) ANN-based controller

4.2. Scenario 1: charging two vehicles with two batteries of different voltages using a common ground assembly

A key objective of this paper is to develop a method enabling the charging of two different battery types with different voltages using a single ground assembly. Figure 8 illustrates this scenario, where a 60 V input voltage (V_{in}) is applied to a DC-DC converter as shown in Figure 8(a). A 72 V battery is charged during the initial 2 seconds, followed by a 48 V battery charge from 2 to 4 seconds. The ANN controller effectively manages power and voltage to charge both battery types, facilitating the charging of two electric vehicles using a single ground-side assembly. The optimized ANN controller effectively achieves this first objective by dynamically adjusting the duty cycle to meet the desired output voltage. As illustrated in Figure 8(b), a duty cycle of 0.5455 is applied to the DC-DC converter during the initial 2 seconds to charge the 72 V battery (boost mode). Subsequently, a duty cycle of 0.4447 is utilized to charge the 48V battery between 2 and 4 seconds (buck mode).

4.3. Scenario 2: maintaining constant output voltage under input voltage fluctuations

This scenario is particularly relevant in contexts where the input voltage to the secondary side of the WPT charger may experience variations. Such fluctuations can arise due to factors like grid instability on the primary side or misalignment between the coils. The second objective of the paper is to maintain the battery charge at a constant voltage despite fluctuations that can change the input voltage V_{in} of the DC-DC converter. Figure 9(a) illustrates scenario 2, where a vehicle is absent between 0 and 0.5 seconds, resulting in a 0 V output voltage V_{out} and a 0-duty cycle as shown in Figure 9(b). Upon vehicle presence at 0.5 seconds, the reference voltage is set to 48 V. When the input voltage V_{in} increases to 70 V at 2 seconds, the ANN controller swiftly adjusts V_{out} to maintain the 48 V reference, accompanied by a corresponding decrease in duty cycle. Conversely, a decrease in V_{in} to 50 V at 3.5 seconds triggers a swift increase in duty cycle to maintain the 48 V output voltage.

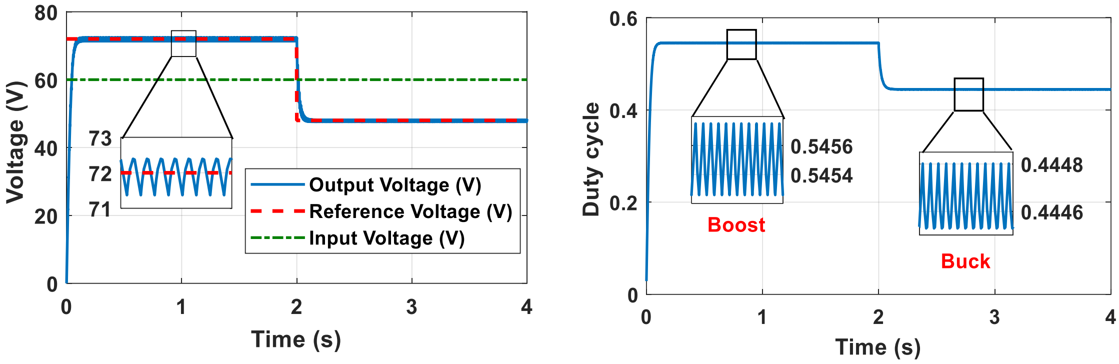

(a) (b)

Figure 8. Output voltage in case of common ground assembly: (a) voltage signals and (b) duty cycle

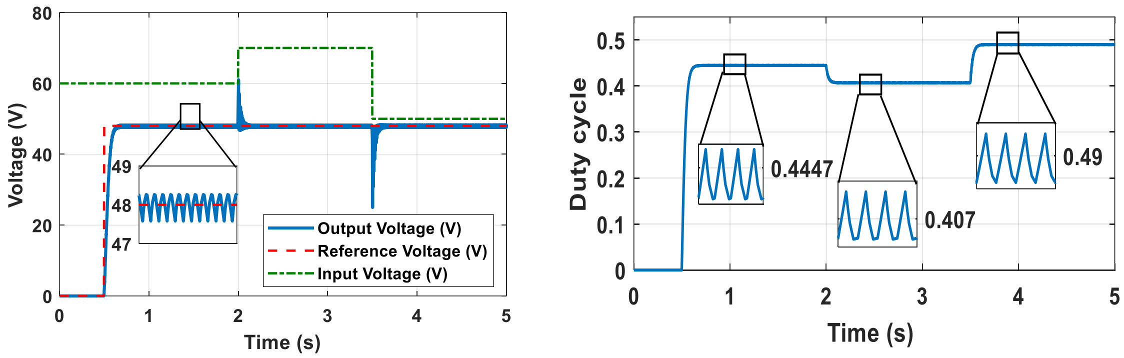

(a) (b)

Figure 9. Output voltage in case of variable input voltage: (a) voltage signals and (b) duty cycle

Figure 10 illustrates the output voltage and current of the inverter. Zoomed-in views of Figures 10(a) and 10(b) demonstrate how adjusting the inverter's output voltage root-mean-square (RMS) value influences the power transmitted from the ground side to the vehicle side. Despite the square-wave nature of the output voltage, the primary coil's current exhibits a sinusoidal waveform due to the filtering effect of the ground-side coil and its associated series capacitor within the resonant LC network. Also, Figure 11 illustrates the input voltage to the vehicle-side rectifier and the corresponding coil current, which are in phase. The input voltage exhibits a square waveform at a frequency of 85 kHz. Due to the filtering effect of the vehicle-side resonant network, the coil current appears as a sine wave at the same resonant frequency.

4.4. Comparison of the proposed approach with other works

A comparative analysis of the proposed ANN-based controller with existing research has been conducted, considering factors such as charging type, controller type, maximum efficiency, robustness, additional sensors required, and versatility. Table 5 provides a comprehensive comparison of this study with previous works on vehicle-side control of WPT chargers. This paper focuses on the CV mode, addressing challenges such as coil misalignment and grid instability. The ANN-based controller employed in this study is characterized by its high efficiency. Also, PI controllers are generally robust under linear conditions, they are less effective in nonlinear scenarios. Nonlinear controllers, on the other hand, are inherently robust to nonlinear environments but can be sensitive to parameter changes and sensor noises. ANN-based controller, however, demonstrates high robustness, particularly in nonlinear and variable conditions. Although the use of ANN may involve higher initial costs due to computational power, their potential benefits in complex and adaptive systems can justify the investment.

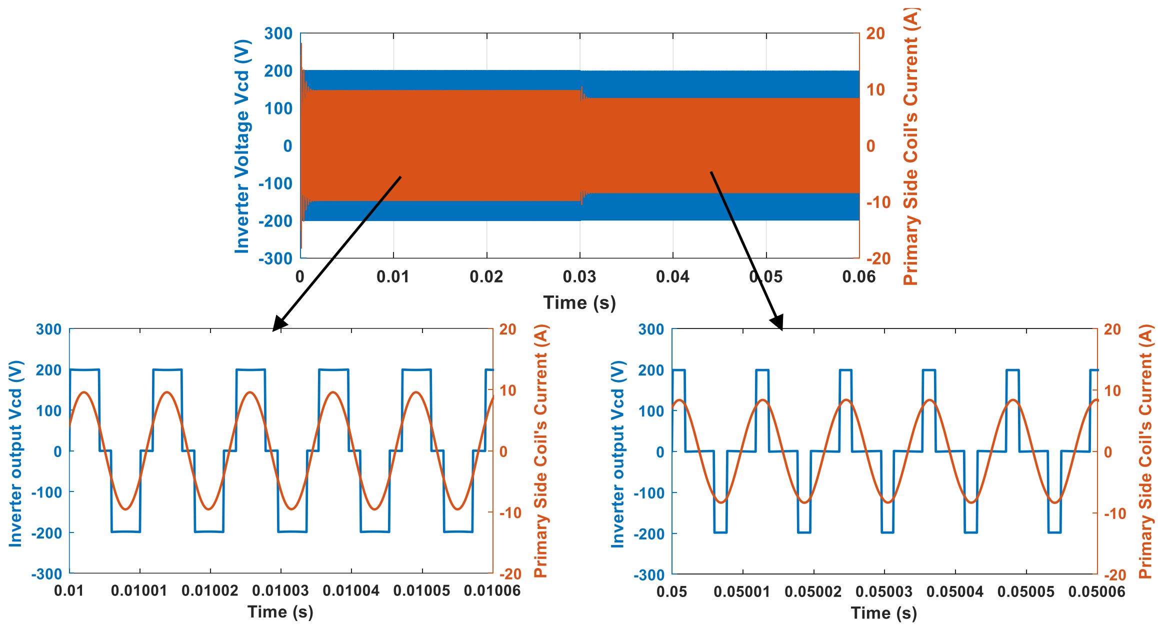

(a) (b)

Figure 10. Primary side coil's current and inverter output voltage and (a) at time 0.01 s and (b) at 0.05 s

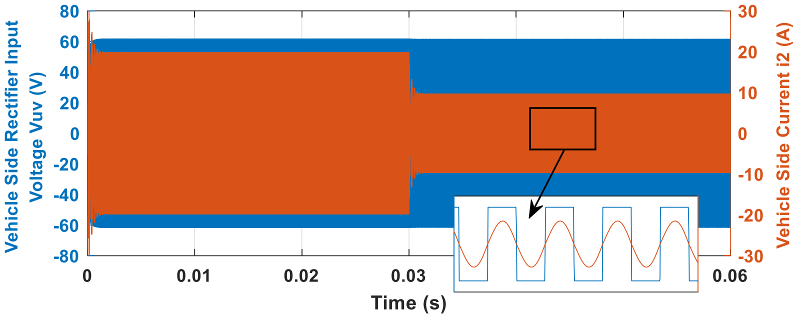

Figure 11. Vehicle side coil's current and rectifier input voltage

Table 5. Performance comparison of the proposed approach with published works

Study	Charging mode	Controller	Maximum efficiency	Robustness	Additional sensors	Versatility
[14]	CC-CV	PI	91.75%	No	No	Low
[15]	CC	PI -OCC	Not provided	No	No	Low
[16]	CC	PI	92%	No	No	Low
[17]	CC-CV	PI	92.9%	No	No	Low
[18]	CV	PI	85.26%	No	No	Low
[19]	CC-CV	H-infinity nonlinear controlle	Not provided	Yes	Yes	Medium
This paper	**CV**	**ANN-based controller**	**90.01%**	**Yes**	**No**	**High**

The proposed ANN-based control strategy offers significant advantages over traditional PI and nonlinear controllers for WPT systems, in the context of electric vehicle battery charging. The ANN controller's ability to eliminate overshoot and significantly reduce residual ripple in the output voltage ensures stable and efficient battery charging. Unlike nonlinear controllers, the ANN-based approach does not require additional sensors, leading to lower costs and system complexity. Moreover, the ANN controller's adaptability to diverse battery voltages and input voltage fluctuations demonstrates its versatility in handling real-world charging scenarios.

This research addresses several existing research gaps, including the ability to charge multiple batteries with diverse voltages using a single ground assembly and the potential of AI to enhance the performance of WPT systems. While the proposed ANN-based control strategy exhibits a slight limitation in terms of system response time due to the computational demands of the ANN controller, this constraint did not significantly impact the overall system efficiency in our study. The system's effectiveness in protecting the battery, a critical component in electric vehicles, is evident through the elimination of overshoot and the substantial reduction of residual voltage ripple during CV charging. These advantages underscore the value of the proposed ANN-based approach for WPT applications. Future research directions include exploring more complex ANN architectures to enhance performance potentially. Additionally, reducing the computational time of the ANN controller would be beneficial, particularly for applications requiring rapid responses such as fast charging. Extensive field testing and validation of the proposed ANN-based control strategy in real-world WPT systems are crucial to assess its practical performance and address potential challenges.

5. CONCLUSION

This paper introduced a novel ANN-based control strategy for vehicle-side WPT chargers, effectively addressing the critical challenge of maintaining constant battery charging voltage under diverse operating conditions. Compared to nonlinear control techniques, the proposed approach offers a more cost-effective and less complex solution. Moreover, the ANN controller's ability to effectively regulate the output voltage, even in the presence of coil misalignment and varying input voltages. The proposed ANN-based controller effectively eliminated overshoot and significantly reduced residual output voltage ripple by 4.33% compared to a conventional PI controller. This highlights the controller's ability to enhance system stability and reduce potential disturbances during battery charging. Additionally, the proposed technique demonstrated robust performance in shared grounding assemblies for EVs with diverse battery voltages. The simulation results validated the proposed technique's performance and accuracy, highlighting its potential for practical implementation in WPT systems. Future research could explore the integration of advanced ANN architectures and optimization techniques to further enhance the controller's performance and address potential limitations. Overall, this paper contributed to the advancement of WPT technology by offering a promising solution for efficient and reliable battery charging in electric vehicles.

REFERENCES

[1] B. Shui, Z. Cai, and X. Luo, “Towards customized mitigation strategy in the transportation sector: an integrated analysis framework combining LMDI and hierarchical clustering method,” *Sustainable Cities and Society*, vol. 107, Jul. 2024, doi: 10.1016/j.scs.2024.105340.

[2] D. M. Papadakis, A. Savvides, A. Michael, and A. Michopoulos, “Advancing sustainable urban mobility: insights from best practices and case studies,” *Fuel Communications*, vol. 20, Sep. 2024, doi: 10.1016/j.jfueco.2024.100125.

[3] R. Ceccato, R. Rossi, and M. Gastaldi, “Low emission zone and mobility behavior: Ex-ante evaluation of vehicle pollutant emissions,” *Transportation Research Part A: Policy and Practice*, vol. 185, Jul. 2024, doi: 10.1016/j.tra.2024.104101.

[4] S. Jagani, E. Marsillac, and P. Hong, “The electric vehicle supply chain ecosystem: changing roles of automotive suppliers,” *Sustainability*, vol. 16, no. 4, Feb. 2024, doi: 10.3390/su16041570.

[5] G. E. M. Abro, S. A. B. M. Zulkifli, K. Kumar, N. El Ouanjli, V. S. Asirvadam, and M. A. Mossa, “Comprehensive review of recent advancements in battery technology, propulsion, power interfaces, and vehicle network systems for intelligent autonomous and connected electric vehicles,” *Energies*, vol. 16, no. 6, 2023, doi: 10.3390/en16062925.

[6] V. Ramakrishnan *et al.*, “A comprehensive review on efficiency enhancement of wireless charging system for the electric vehicles applications,” *IEEE Access*, vol. 12, pp. 46967–46994, 2024, doi: 10.1109/ACCESS.2024.3378303.

[7] C. Thangavel, V. Krishnamoorthy, and V. Jayasankar, “An approach of dynamic wireless charging structure for an electric vehicle based on mutual inductance calculation,” *International Journal of Power Electronics and Drive Systems*, vol. 15, no. 3, pp. 1564–1572, 2024, doi: 10.11591/ijpeds.v15.i3.pp1564-1572.

[8] D. Purushothaman, N. R, and V. K. Ramachandramurthy, “Charging ahead: unlocking the potential of constant voltage and constant current modes in WPT for EVs,” *Journal of Energy Storage*, vol. 96, 2024, doi: 10.1016/j.est.2024.112603.

[9] K. Obaideen, L. Albasha, U. Iqbal, and H. Mir, “Wireless power transfer: applications, challenges, barriers, and the role of AI in achieving sustainable development goals - a bibliometric analysis,” *Energy Strategy Reviews*, vol. 53, 2024, doi: 10.1016/j.esr.2024.101376.

[10] T. A. Vu, C. Van Pham, W. Tran, A. V. Pham, and C. S. Gardner, “Wireless power and data transfer through carbon composite using a common inductive link,” *International Journal of Power Electronics and Drive Systems*, vol. 11, no. 3, pp. 1441–1448, 2020, doi: 10.11591/ijpeds.v11.i3.pp1441-1448.

[11] M. El Ancary *et al.*, “Control of a wireless power transfer charger powered by renewable energies,” in *2024 4th International Conference on Innovative Research in Applied Science, Engineering and Technology, IRASET 2024*, 2024, pp. 1–6, doi: 10.1109/IRASET60544.2024.10548631.

[12] A. Lassioui, M. El Ancary, Z. El Idrissi, H. El Fadil, K. Rachid, and A. Rachid, “Primary-side indirect control of the battery charging current in a wireless power transfer charger using adaptive hill-climbing control technique,” *Processes*, vol. 12, no. 6, 2024, doi: 10.3390/pr12061264.

[13] Z. Liu, T. Li, S. Li, and C. C. Mi, “Advancements and challenges in wireless power transfer: a comprehensive review,” *Nexus*, vol. 1, no. 2, 2024, doi: 10.1016/j.ynexs.2024.100014.

[14] B. Bhavsingh, S. B. Gotluru, M. Bhukya, and R. Bhukya, “Investigation of 1.5 kW secondary side power controlled method in a inductive wireless power transfer system,” *International Journal of Power Electronics and Drive Systems*, vol. 15, no. 2, pp. 670–684, 2024, doi: 10.11591/IJPEDS.V15.I2.PP670-684.

[15] B. Chen, G. Yao, L. Zhou, and M. Zhao, “Study on secondary side control of wireless power transfer based on LCC compensation,” in *2021 IEEE 3rd International Conference on Circuits and Systems, ICCS 2021*, 2021, pp. 196–202, doi: 10.1109/ICCS52645.2021.9697313.

[16] B. Bhavsingh, G. S. Babu, B. Mangu, and R. Bhukya, "A receiver-side power control method for series-series magnetic topology in inductive contactless electric vehicles battery charger application," *International Journal of Advances in Applied Sciences*, vol. 12, no. 3, pp. 234–249, 2023, doi: 10.11591/ijaas.v12.i3.pp234-249.

[17] H. Zhang, Y. Chen, D. H. Kim, Z. Li, M. Zhang, and G. Li, "Variable inductor control for misalignment tolerance and constant current/voltage charging in inductive power transfer system," *IEEE Journal of Emerging and Selected Topics in Power Electronics*, vol. 11, no. 4, pp. 4563–4573, 2023, doi: 10.1109/JESTPE.2023.3281891.

[18] S. Cetin and V. Yenil, "High efficiency constant voltage control of LC/S compensated wireless power transfer converter based on pulse density modulation control," *International Journal of Electronics*, vol. 110, no. 1, pp. 54–72, 2023, doi: 10.1080/00207217.2021.2001875.

[19] J. Zhao, Z. Zhang, and K. Zhang, "Control design and parameter optimization on secondary side of electric vehicle wireless charging system based on H∞ nonlinear controller," *Diangong Jishu Xuebao/Transactions of China Electrotechnical Society*, vol. 37, no. 3, pp. 566–577, 2022, doi: 10.19595/j.cnki.1000-6753.tces.201591.

[20] SAE International, "Wireless power transfer for light-duty plug-in/electric vehicles and alignment methodology," *SAE International*. https://www.sae.org/standards/content/j2954_202010/ (accessed Jan. 22, 2024).

[21] R. Vidya and B. K. Keshavan, "Optimizing performance parameters of stationary wire free power transfer circuit," *International Journal of Power Electronics and Drive Systems*, vol. 14, no. 3, pp. 1309–1321, 2023, doi: 10.11591/ijpeds.v14.i3.pp1309-1321.

[22] M. Konghirun, S. Nutwong, A. Sangswang, and N. Hatchavanich, "Design of the transmitter coil used in wireless power transfer system based on genetic algorithm," *International Journal of Power Electronics and Drive Systems*, vol. 14, no. 4, pp. 2307–2318, 2023, doi: 10.11591/ijpeds.v14.i4.pp2307-2318.

[23] A. Lassioui *et al.*, "Output feedback control of a WPT charger based on sliding mode and high Gain observer," in *2024 4th International Conference on Innovative Research in Applied Science, Engineering and Technology, IRASET 2024*, 2024, pp. 1–6, doi: 10.1109/IRASET60544.2024.10548398.

[24] F. Z. Belhaj *et al.*, "Modelling and sliding mode control of a wireless power transfer system for BEV charger," *International Journal of Modelling, Identification and Control*, vol. 34, no. 2, 2020, doi: 10.1504/ijmic.2020.10032860.

[25] J. Jayachandran and S. Malathi, "Improved power quality buck boost converter for SMPS," *International Journal of Electrical and Computer Engineering*, vol. 9, no. 2, pp. 789–801, 2019, doi: 10.11591/ijece.v9i2.pp789-801.

[26] H. Aly, A. K. Al-Ali, and P. N. Suganthan, "Boosted multilayer feedforward neural network with multiple output layers," *Pattern Recognition*, vol. 156, 2024, doi: 10.1016/j.patcog.2024.110740.

BIOGRAPHIES OF AUTHORS

Marouane El Ancary received his Agrégation degree in electrical engineering from the Ecole Normale Supérieure de l'Enseignement Technique (ENSET) at Mohammed V University in Rabat, Morocco, in 2012. He also earned an MS degree in electronic engineering from Abdelmalek Essaadi University in Tetouan, Morocco, in 2021. He is currently pursuing a PhD in electrical engineering at the ISA Laboratory at National School of Applied Sciences (ENSA), Ibn Tofail University, Kenitra, Morocco. His primary research areas include electric vehicles, wireless power transfer chargers, control and optimization, and the application of artificial intelligence in control systems. He can be contacted at email: marouane.elancary@gmail.com.

Abdellah Lassioui received his diploma of state engineer in electrical engineering from The University of Sciences and Techniques, Tangier, Morocco in 2015. He received his PhD in automatic control in 2021, Université Ibn Tofail, Kenitra, Morocco. He is currently with the ISA Laboratory. Since 2022, he has been, successively assistant professor at the Ecole Nationale des Sciences Appliquées, Université Ibn Tofail, Kenitra, Morocco. His current research interests include the fields of nonlinear control of power electronic systems, electric vehicles, and wireless power transfer charging for electric vehicles. He has co-authored over 40 journal and conference papers. He can be contacted by email: Abdellah.lassioui@uit.ac.ma.

Hassan El Fadil received his BS degree in electronics, the Agrégation degree in electrical engineering, the MS degree in automatic control and the PhD degree in automatic control from the Ecole Mohammadia d'Ingénieurs, Université Mohammed V, Rabat, Morocco, in 1994, 1999, 2003 and 2008, respectively. Since 2011, he has been, successively assistant professor, Habilitated professor and full professor in the Ecole Nationale des Sciences Appliquées, Université Ibn Tofail, Kenitra, Morocco. He is currently with the ISA Laboratory. His research interest includes nonlinear and adaptive control, power converters and electric motors control, renewable energy, distributed energy resources, smart grid, and electric vehicles. He has published over 160 journal/conference papers. He can be contacted at email: elfadilhassan@yahoo.fr.

Anwar Hasni was born in 2000 in Errachidia, Morocco, and graduated with a bachelor's degree in mathematical sciences. He then studied at the National School of Applied Sciences (ENSA) at Ibn Tofail University in Kenitra, where he obtained a state diploma in electrical engineering in 2023. He is currently a doctoral student and researcher in the advanced systems engineering Laboratory at ENSA Kénitra. He can be contacted at email: anwar.hasni@uit.ac.ma.

Yassine El Asri received the master of research degree in electrical engineering from the ENSET of Rabat, Morocco, in 2020. He is currently working toward the Ph.D. degree in the Advanced Systems Engineering Laboratory at the ENSA Kenitra, Morocco. His main area of research is renewable energy emulators and storage systems. He can be contacted at email: elasriyassine@yahoo.com.

Zakariae El Idrissi received his State Engineer Diploma in electrical engineering from National School of Applied Sciences (ENSA), OUJDA, Morocco, in 2014. He received the PhD degree in automatic control of electrical systems from Ibn Tofail University, Kenitra, Morocco, in 2021. His research interests include optimization, observation and control of energy systems used in electric vehicles. He can be contacted at email: zakariae.elidrissi@gmail.com.